



Universiteit  
Leiden  
The Netherlands

## **Rapid aggregation of therapeutic monoclonal antibodies by bubbling induced air/liquid interfacial and agitation stress at different conditions**

Sreenivasan, S.; Jiskoot, W.; Rathore, A.S.

### **Citation**

Sreenivasan, S., Jiskoot, W., & Rathore, A. S. (2021). Rapid aggregation of therapeutic monoclonal antibodies by bubbling induced air/liquid interfacial and agitation stress at different conditions. *European Journal Of Pharmaceutics And Biopharmaceutics*, 168, 97-109. doi:10.1016/j.ejpb.2021.08.010

Version: Publisher's Version

License: [Licensed under Article 25fa Copyright Act/Law \(Amendment Taverne\)](#)

Downloaded from: <https://hdl.handle.net/1887/3243946>

**Note:** To cite this publication please use the final published version (if applicable).



# Rapid aggregation of therapeutic monoclonal antibodies by bubbling induced air/liquid interfacial and agitation stress at different conditions

Shravan Sreenivasan<sup>a</sup>, Wim Jiskoot<sup>b</sup>, Anurag S. Rathore<sup>a,\*</sup>

<sup>a</sup> Department of Chemical Engineering, Indian Institute of Technology Delhi, India

<sup>b</sup> Division of BioTherapeutics, Leiden Academic Centre for Drug Research (LACDR), Leiden University, The Netherlands

## ARTICLE INFO

### Keywords:

Aggregation  
Agitation  
Bubbling  
Interfacial stress  
Monoclonal antibody  
Turbidity

## ABSTRACT

Degradation of therapeutic monoclonal antibodies (mAb) due to interfacial agitation through air bubbling was investigated. Samples containing mAb in phosphate buffered saline were subjected to rapid bubbling by using a peristaltic pump at an air flow rate of 11.5 mL/min. Samples were analyzed by visual observation, UV–Vis, fluorescence, circular dichroism and infrared spectroscopy, size-exclusion chromatography (SEC), dynamic light scattering, microscopy, and cell-based activity assays. The stressed samples showed increasing turbidity with bubbling time, with mAb1 showing a protein loss of 53% in the supernatant at the latest time point (240 min), indicating formation of sub-visible and visible aggregates. Aggregate rich samples exhibited altered secondary structure and higher hydrophobicity with 40% reduction in activity. The supernatants of the stressed samples showed unchanged secondary and tertiary structure without the presence of any oligomers in SEC. Furthermore, the impact of various factors that could affect aggregation was investigated and it was found that the extent of aggregation was affected by protein concentration, sample volume, presence of surfactants, temperature, air flow rate, and presence of silicone oil. In conclusion, exposure to air/liquid interfacial stress through bubbling into liquid mAb samples effectively generated sub-visible and visible aggregates, making air bubbling an attractive approach for interfacial stress degradation studies of mAbs.

## 1. Introduction

Therapeutic monoclonal antibodies (mAb) are used for effective management of a variety of difficult-to-treat diseases [1]. The inherent instability of mAbs is a major challenge during drug product development, because degradation, such as aggregation and fragmentation, can occur during various stages of cell culture, downstream processing, formulation, transportation, storage, handling and administration [2]. Aggregates can differ in size, shape, morphology and structure [2,3]. Monitoring, analysis and control of stability is a critical challenge, as the degradation of mAb may result in reduced activity, limited shelf life, low process yield and hindrance in the development of novel applications [3,4]. Moreover, aggregates might cause adverse immune responses,

such as anaphylaxis and neutralizing antibody formation, leading to loss of activity or neutralization of endogenous proteins [1,5]. So, there is continued interest in understanding the stability of mAb (and other biotherapeutic) products as well as developing strategies for enhancing it [6,7]. The impact of aggregation on immunogenicity and function of the biotherapeutic also remains an important topic of research [1,2,5].

Protein aggregation is influenced by a variety of factors –besides intrinsic properties of the protein–, including buffer composition, protein concentration, temperature, mechanical stress, and interfacial surfaces [2,7]. Exposure of mAbs to different interfaces is unavoidable, as it occurs in the form of different solid/liquid, liquid/liquid and air/liquid surfaces [8] during different stages of manufacturing, shipment and handling [8–11] and can result in the formation of aggregates of various

**Abbreviations:** ADCC, antibody dependent cell-mediated cytotoxicity; AI, aggregation index; ANS, 1-anilino-8-naphthalenesulfonate; ATR, attenuated total reflectance; AUC, area under the curve; CDC, complement dependent cytotoxicity; CD, circular dichroism; DLS, dynamic light scattering; FTIR, Fourier transform infrared; HPLC, high performance liquid chromatography; IgG, immunoglobulin; LDH, lactate dehydrogenase; mAb, monoclonal antibodies; MTS, 3-(4, 5-dimethylthiazol-2-yl) 5-(3-carboxymethoxyphenyl)-2-(4-sulphonyl)-2H-tetrazolium salt; OD, optical density; PBMC, peripheral blood mononuclear cells; PBS, phosphate buffered saline; PMS, phenazine methosulfate; PS, polysorbate; SEC, size-exclusion chromatography;  $\lambda_{max}$ , maximum emission intensity wavelength.

\* Corresponding author at: Department of Chemical Engineering, Coordinator, DBT Center of Excellence for Biopharmaceutical Technology, Indian Institute of Technology Delhi, Hauz Khas, New Delhi, 110016, India.

E-mail address: [asrathore@biotechmz.com](mailto:asrathore@biotechmz.com) (A.S. Rathore).

<https://doi.org/10.1016/j.ejpb.2021.08.010>

Received 21 May 2021; Received in revised form 6 August 2021; Accepted 19 August 2021

Available online 28 August 2021

0939-6411/© 2021 Elsevier B.V. All rights reserved.

size ranges [12,13]. Air/liquid interfaces are encountered in the form of head space and air bubbles [14], and can occur along with agitation [8]. Various studies have showed that combined occurrence of interfacial stress and agitation is highly detrimental to the stability of mAbs [7,9,10,12] and such stresses are known to exist in several process operations, including centrifugation, sparging, mixing, pumping, filtration, shaking, filling, packaging, transportation, and handling during clinical administration [7–9].

The mechanism by which the exposure of mAb to interfacial surfaces and agitation results in aggregation is not so well established [8]. However, one of the theories states that in presence of air/liquid interfacial stress, proteins adsorb to the hydrophobic air/liquid interface that results in (partial) unfolding and, consequently, exposure of hydrophobic patches and this instigates partial unfolding of the molecule followed by interaction with other (folded or unfolded) monomers to form aggregates [8,13]. However, there are other proposed mechanisms where the proteins remain in native like conformation at the interface [14]. The combination of mechanical shear due to agitation and interfacial surfaces enhances rapid exchange of aggregation nuclei from the interface to the bulk and transfer of native proteins from bulk to interface, thereby accelerating interactions among proteins in the native and partially unfolded state, and promoting aggregation [8,13].

The impact of air/liquid interfacial stress and its combination with agitation on samples containing therapeutic immunoglobulins (IgGs) requires deeper investigation [8,9,12]. Aggregation can be accelerated by stressing the mAb samples externally by rapid bubbling-induced agitation [15]. Moreover, forced degradation strategies can give insights into the type of aggregates, their structure, aggregation rate, protein activity and reversibility of the aggregation process in a very short time span. Therefore, such strategies could be helpful during molecule screening, formulation development, comparability testing and analytical method development. Furthermore, forced degradation studies can help in gaining insights about the stability profile of the protein during accidental exposure of the stress, establishing shelf life and determination of its degradation profile [15]. Researchers have used a variety of specialized equipment for analysing protein degradation [8,12–14,16,17]. However, there is a lack of guidelines or recommendations to assess the impact of such kind of stresses [8,12,15].

In this paper, we present a simple in-house set-up comprising a peristaltic pump, silicone tubing, an air filter, and a syringe needle to induce combined air/liquid interfacial stress and agitation to mAb samples. The term ‘interfacial agitation through bubbling’ is used throughout this study and it refers to rapid bubbling-induced agitation that serves as source of mechanical shear and constant renewal of interfacial surfaces. The set-up for bubbling allowed us to subject the samples to accelerated stress through rapid generation of air bubbles at 37 °C. A temperature of 37 °C was chosen as it could represent an elevated temperature a mAb product could be exposed to, e.g., during transportation and handling. The study involved the use of three IgGs (two IgG1s and one IgG4). All samples were subjected to stress and characterized in terms of particle size, protein structure, and activity by using a wide array of analytical techniques including turbidity, visual inspection, UV–Vis spectroscopy, size-exclusion chromatography (SEC), dynamic light scattering (DLS), bright-field microscopy, fluorescence spectroscopy, circular dichroism (CD) spectroscopy, attenuated total reflectance-Fourier transform infrared (ATR-FTIR) spectroscopy and cell-based activity assays. Moreover, the impact of various factors, such as protein concentration, sample volume, temperature, bubbling rate, and presence of excipients was evaluated.

## 2. Materials and methods

### 2.1. Reagents

All the chemicals were of high purity analytical grade. The buffers used were prepared in-house and filtered through a 0.22 µm nylon

membrane filter (Pall Life Sciences, NY, USA) followed by degassing. Polysorbate 80 (PS80), PS20 and silicone oil were of pharmaceutical grade.

### 2.2. IgG

Two humanized IgGs, mAb1 (IgG1) and mAb2 (IgG1) were obtained from a major biopharmaceutical producer in India. Another IgG (mAb3), an IgG4 provided by the same company, was used but the details of the molecule were not revealed to us. The stock of IgGs was present in buffer consisting of sodium phosphate and sodium chloride and was stored at a concentration of 10 mg/mL. Samples containing mAb were buffer exchanged to phosphate buffered saline (PBS) using preparative size-exclusion chromatography with Sephadex G-25 resin (GE Healthcare Biosciences, Pittsburgh, PA, USA) packed into a Tricon column (100 × 10 mm) on an ÄKTA Purifier system (GE Healthcare Europe GmbH, Freiburg, Germany). PBS was made in our lab and it consisted of 2.7 mM KCl, 10 mM phosphate and 137 mM NaCl. The buffer had a pH of 7.4. The sample containing IgG and buffers used in the study were filtered using a nylon membrane filter having a cut-off of 0.22-µm (Pall Life Sciences, Port Washington, NY, USA).

### 2.3. Stressing of samples containing IgG

500 µL of sample containing 1 mg/mL of IgG in PBS was taken in a 2-mL Eppendorf tube and maintained at 37 °C in a dry bath (GeNei, India). A Dispo Van syringe needle (0.8 mm inner diameter) and a 0.2 µm pore size exhaust filter (Midisart Sartopore Air, Sartorius, Germany) were attached to both ends of a silicone tube (L/S 16; 3.1 mm inner diameter and 30 cm long). The silicone tubing was attached to a peristaltic pump (Masterflex L/S 2000, Germany) and the tip of the needle was inserted into the IgG sample in the Eppendorf tube of 2 mL capacity (Fig. 1). The pump was operated at 5 rpm to induce rapid bubbling, which was the source of air/liquid interfacial agitation stress to the IgG sample. The air flow rate and the average bubble diameter were calculated as described in Supporting Information sections 1 and 2. The air flow rate at 5 rpm was calculated as 11.5 mL/min. Subsequently, the air flow rates at 1, 2.5 and 7.5 rpm were calculated as 1.60, 2.75 and 17.25 mL/min, respectively. The average bubble diameter was calculated as 1.9 mm (SI section 2). A visual representation of generated air bubbles in a conical flask

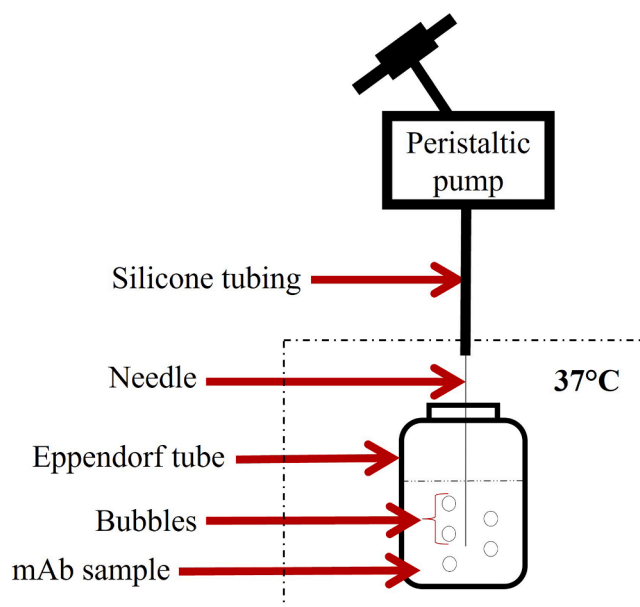


Fig. 1. Schematic picture of the experimental set-up for the generation of air/liquid interfacial agitation by introducing air bubbles into mAb samples.

containing water is shown in the [Supplementary Information](#) (SI Fig. 1a). The pump was operated at 5 rpm, unless stated otherwise. Aseptic procedures such as usage of autoclaved tubing, syringe needles and usage of filtered samples were followed. Analysis of aggregates was performed at various time points up to 240 min. Samples not subjected to interfacial agitation through bubbling stress and incubated for stressing time and temperature in the presence of dipped needle were used as the controls. In order to access the impact of various conditions, the samples were stressed at different temperature, air flow rate, volume, presence of various excipients and silicone oil, the details of which are mentioned in the results section. Unless stated otherwise, 500  $\mu\text{L}$  of 1 mg/mL of mAb1, mAb2 or mAb3 in PBS were subjected to interfacial agitation by bubbling at an air flow rate of 11.5 mL/min at 37 °C. The analysis was performed at various time points up to 4 h.

#### 2.4. Visual observation

The samples subjected to interfacial agitation stress and controls were visually inspected, photographed and were marked from 0 (visibly clear) to +++ (highly turbid) based on visual observation. Vials containing only PBS (blank) was marked as 0 and taken as the reference.

#### 2.5. UV–Vis spectroscopy

UV–Vis spectroscopy of the samples was performed by using a Multiskan GO UV/Vis spectrophotometer (Thermo Fisher Scientific, Waltham, MA, USA). 200  $\mu\text{L}$  of samples were loaded onto a 96 well-plate. The spectra were recorded from 280 to 360 nm and were corrected for the suitable buffers. The optical density (OD) at 350 nm was used as an indication of turbidity. The aggregation index (AI) was calculated using the OD of the sample at 280 nm and 350 nm (equation (1)). AI is a parameter that is a measure of aggregate content, though it does not provide any details of particle size distribution. The stressed samples were centrifuged at 8000 rpm for 10 min, followed by careful separation of pellet and the supernatant. The amount of protein in the supernatant was analyzed as protein loss (%), which was calculated using equation (2), where ‘Initial  $A_{280}$ ’ is the absorbance of sample at 280 nm before subjecting it to stress and ‘Final  $A_{280}$ ’ is the absorbance of supernatant at 280 nm after the sample has been subjected to stress.

$$\text{AI} = \frac{\text{OD at 350nm}}{(\text{OD at 280nm} - \text{OD at 350nm})} \times 100 \quad (1)$$

$$\% \text{Protein loss} = \frac{(\text{Initial } A_{280} - \text{Final } A_{280})}{(\text{Initial } A_{280})} \times 100 \quad (2)$$

#### 2.6. Size-exclusion chromatography (SEC)

The monomer, aggregates and fragments in the supernatant were analyzed by using SEC. A Superdex 200 (10 mm wide and 300 mm long) column (GE Healthcare Biosciences, Pittsburgh, PA, USA) mounted on a Dionex Ultimate 3000 High-performance liquid chromatography (HPLC) unit (Thermo Scientific, Sunnyvale, CA, USA). The mobile phase consisted of 50 mM phosphate buffer filtered using a 0.22- $\mu\text{m}$  cut off nylon membrane filter. The HPLC method consisted of isocratic elution for 45 min at a flow rate of 0.5 mL/min. Detection was performed by monitoring the UV absorbance at 280 nm. Similarly, the fragments were quantified using a Superdex 75 (GE Healthcare Biosciences, Pittsburgh, PA, USA) column with the same instrument, mobile phase and method as mentioned for Superdex 200, used for analysing the aggregates. The percentage loss in area under the curve (AUC) of supernatants of samples subjected to stress was calculated using equation (3) using the AUC obtained from Superdex 200 column.

$$\% \text{AUC loss} = \left( \frac{\text{AUC of unstressed sample} - \text{AUC of supernatant}}{\text{AUC of unstressed sample}} \right) \times 100 \quad (3)$$

#### 2.7. Dynamic light scattering (DLS)

DLS was performed by using a Zetasizer Nano ZS 90 (Malvern Instruments, UK) particle size analyzer consisting of a 633-nm He-Ne laser. 60  $\mu\text{L}$  of sample was loaded onto the cuvette and triplicate sample analysis was performed at 25 °C with an equilibration time of 120 s. The Z-average diameter was calculated from the correlation function using the Dispersion Technology Software (version 4.20, Malvern).

#### 2.8. Automated microscopic analysis

Aggregates were visualized by using a Cytell Cell Imaging System (GE Healthcare, UK). A C-chip (NanoEntek, Lebtch, UK) containing 20  $\mu\text{L}$  of sample subjected to interfacial agitation stress was loaded into the instrument. The C-chip is a disposable plastic hemocytometer, and it enables uniform loading of samples. Exposure and gating were adjusted manually. The Automated Imaging BioApp was used for automatic acquisition of numerous brightfield images. The acquired images had a resolution of 1920 (width)  $\times$  1440 (height) and a scale by pixel ratio of 1.1 ( $\mu\text{m}/\text{pixels}$ ) and were analyzed by using MATLAB-based image processing, in which the images obtained from the microscope are called in for image analysis on MATLAB. The images are processed through several steps, starting from conversion to grayscale. It was followed by determining the number of pixels corresponding to each color code from 0 to 255, where 0 represents black and 255 represents white. The pixel-color distribution and was plotted, and was used to segregate the aggregates, background and hemocytometer lines using suitable thresholding as the aggregates are dark colored and it covered the left portion of the peak while the background and particle boundary included the peak and the right side of it. Following thresholding, morphological operations were performed to improve the images and the particles output binary images were labeled and the area corresponding to each label was determined. The scale by pixel ratio was used to normalize the data from pixel to metric format. From the extracted data, size distribution of aggregates was obtained.

#### 2.9. CD spectroscopy

CD measurements were performed on JASCO J-1500 spectropolarimeter (Tokyo, Japan). For obtaining far-UV spectra, the supernatant containing 0.2 mg/mL of IgG was analyzed in the range of 190–260 nm at 25 °C with a 0.1 cm path length quartz cell at a scan speed of 100 nm/min. Near-UV CD spectra were recorded in the range of 250–340 nm at 25 °C using a 1 cm path length quartz cell at a scan speed of 100 nm/min with a sample concentration of 1 mg/mL. Three spectra were scanned, averaged, and plotted after subtracting the buffer baseline for both far and near-UV spectra.

#### 2.10. Fluorescence spectroscopy

Fluorescence spectroscopy was performed on a Cary Eclipse spectrophotometer (Agilent Technologies). For measuring intrinsic fluorescence, 200  $\mu\text{L}$  of sample (0.2 mg/mL) was loaded onto a black fluorescence plate (Greiner Bio-One, Kremsmünster, Austria), and the emission spectra were recorded at a temperature of 25 °C in the range of 290–400 nm with an excitation wavelength of 280 nm. Extrinsic fluorescence spectra were obtained using a fluorescent dye, 1-anilino-8-naphthalenesulfonate (ANS) by recording the emission spectra of the samples from 400 to 600 nm at an excitation wavelength of 350 nm. 10  $\mu\text{M}$  of ANS was added and the samples were incubated for 120 min at 25 °C in dark. Different concentration of ANS and incubation time was



tested as a preliminary study.

### 2.11. ATR-FTIR

ATR-FTIR spectroscopy measurements were made using an ATR accessory equipped with a single bounce diamond crystal on a Thermo Fisher Scientific Nicolet iS50 FT-IR spectrometer. 20  $\mu\text{L}$  of sample containing aggregates, monomer, supernatant, or the collected pellet was loaded onto the surface of the ATR crystal. The analysis was performed at 25 °C and the spectra were acquired over a range of 4000 to 400  $\text{cm}^{-1}$ . The number of scans was 256 at a resolution of 2  $\text{cm}^{-1}$ . The acquired spectra were normalized to nullify the effect of concentration. Following normalization, the subtraction of blank, obtaining second derivative and smoothing was done. The spectra in the range of 1700–1600  $\text{cm}^{-1}$  was then analyzed to assess the changes in secondary structure.

### 2.12. Cell-based assays

Antibody dependent cell-mediated cytotoxicity (ADCC) and complement dependent cytotoxicity (CDC) assays of samples containing stressed mAb2 were performed on a Raji cell line, which was procured from National Centre for Cell Science, Pune, India. The cells were cultured and maintained at 37 °C and 5%  $\text{CO}_2$  in RPMI 1640 medium (Gibco). The medium was supplemented with 10% foetal bovine serum (Gibco) and 1% Pen-strep (Thermo Fisher Scientific, Waltham, MA, USA).

For the ADCC assay, freshly isolated peripheral blood mononuclear cells (PBMC) were used as the effector cells with cultured Raji cells as the target cells. Approval was taken from Institution Ethics Committee, IIT Delhi (Reference No. P-041) for the isolation of human PBMCs. The protocol for the isolation of human PBMCs was followed as mentioned in the cited literature [18]. PBMCs and Raji cells were co-cultured at a cell concentration of  $2.5 \times 10^5$  and  $1 \times 10^4$  cells per well in RPMI 1640 media in 96 well plate. mAb2 was subjected to interfacial agitation for different time points till 240 min followed by 2x, 4x and 8x serial dilution (v/v). Samples were then seeded into the co-cultures and incubated overnight at 37 °C. Following incubation, the cell culture supernatants and blank were isolated and subjected to lactate dehydrogenase (LDH) activity using an LDH cytotoxicity assay kit (Thermo Fisher Scientific, Waltham, MA, USA) as per the manufacturer's protocol. The absorbance at 490 nm was measured by Epoch microplate reader (BioTek Instruments). Percentage of cytotoxicity was calculated, and the relative potency was determined by using a parallel logistic (4-parameter fit) assay on PLA 3.0 bioassay software.

For the CDC assay, wells of 96-well plates containing  $2.5 \times 10^5$  Raji cells per well and human serum (Millipore Corporation; Cat# S1-100 mL) were dosed with samples subjected to stress for different time points at serial various serial dilutions following its incubation overnight at 37 °C at 5%  $\text{CO}_2$ . Following incubation, CDC was determined by adding 3-(4,5-dimethylthiazol-2-yl) 5-(3-carboxymethoxyphenyl)-2-(4-sulphonyl)-2H-tetrazolium salt (MTS)-phenazine methosulfate (PMS). MTS (2.0 mg/mL) and PMS (0.92 mg/mL) were added in a ratio of 10:1 v/v (20  $\mu\text{L}$  per well), and the plates were incubated for 3 h at 37 °C. The absorbance, representing formazan production, was calculated by subtracting the background absorbance from the total absorbance. Data analysis was performed by parallel line assay method by four-parametric logistic fit (PLA 3.0 bioassay software). For both ADCC and CDC, the untreated control sample was taken as the reference standard. In PLA 3.0 software, the potency of the reference standard was taken as 1 IU/mL and was compared with samples subjected to stress. Stressed samples, supernatants and controls were used for both ADCC & CDC. The samples were analyzed in triplicates with suitable blanks.

### 2.13. Impact of various parameters

The effect of interfacial agitation through bubbling was investigated

for different parameters such as mAb concentration (1, 2, 4 and 8 mg/mL), sample volume (0.125, 0.25, 0.5, 1 and 2 mL), temperature (4, 25, 37, 50 and 75 °C), bubbling rate (1, 2.5, 5 and 7.5 rpm), and presence of additives (polysorbate (PS) 80, PS20 and silicone oil). The samples were subjected to stress in the same Eppendorf tube of same volume in all the cases. The samples were stressed for 240 min and were investigated for protein loss in the supernatant, visual observation, and turbidity.

## 3. Results

An air/liquid interfacial agitation through bubbling was introduced by passing air through the solution containing mAb. The samples incubated at 37 °C and not subjected to bubbling were used as controls. The analytical characterisation details of mAb1 are depicted throughout the study, unless stated otherwise. The results are depicted as mean of samples analyzed at least in duplicate.

### 3.1. Visual observation

The samples after being stressed for different time points from 0 to 240 min is shown in Fig. 2a. Samples not subjected to any stress was clear and devoid of any visible aggregates. The samples stressed for 30 min were slightly opalescent. Furthermore, the visual opalescence kept increasing till 240 min. Hence, in the Fig. 2a, the sample not subjected to any stress was marked as 0, followed by marking the samples as 1 to 4 with increase in time. The arbitrary marking of the samples, as 0, +, ++ and +++, for clearly visible (0) to high turbidity (+++) resulted in turbidity-time curves as shown in SI Fig. 1b. The data at each time point was noted as the average of observations made by two separate users for three samples that were the triplicates. Further, the control samples were clear and did not show visible particles. The increase in turbidity for stressed samples was due to the formation of visible and sub-visible aggregates, which was further confirmed and quantified in the subsequent analytical characterization.

### 3.2. UV/Vis spectroscopy

The turbidity of stressed samples determined by measuring the OD at 350 nm at different time points is shown in Fig. 2b. The trend of increasing turbidity with time was similar to that of visual observation. The change in AI for samples subjected to stress is shown in Fig. 2c. Here too, the AI increased from 10.1 at 30 min to 50.5 at 240 min. The changes in AI for mAb2 and mAb3 are shown in Fig. 2d. It was found that all the 3 mAbs followed a similar trend, although the absolute values differed.

The percentage of protein loss in the supernatant (cf. section 2.5) along with the AI is shown in Fig. 2c. The mAb1 sample stressed for 30 min showed 9.5% protein loss, which increased with incubation time to 54.3% for the sample stressed for 240 min. The change in the trend of AI, turbidity and protein loss indicates that the soluble proteins in the sample were converted into visible and sub-visible aggregates. All the 3 mAbs under consideration showed a similar trend for the protein loss, mAb3 being the most unstable one (SI Fig. 2). The control samples did not show any increase in turbidity, AI and protein loss. This shows that the agitation through bubbling at 37 °C is highly detrimental to the stability of the mAbs. The size of the aggregates formed in the stressed samples was studied by using SEC, DLS and microscopy-based image analysis.

### 3.3. Size-based characterization of stressed mAb samples

The observed SEC chromatogram shows, besides the monomer, the presence of oligomers and fragments, with a representation shown in SI Fig. 3a. Two SEC columns namely, Superdex 200 and Superdex 75, were used in this study. In the case of Superdex 200 column, the elution profile corresponding to mAb1 monomer was obtained at 24.98 min,

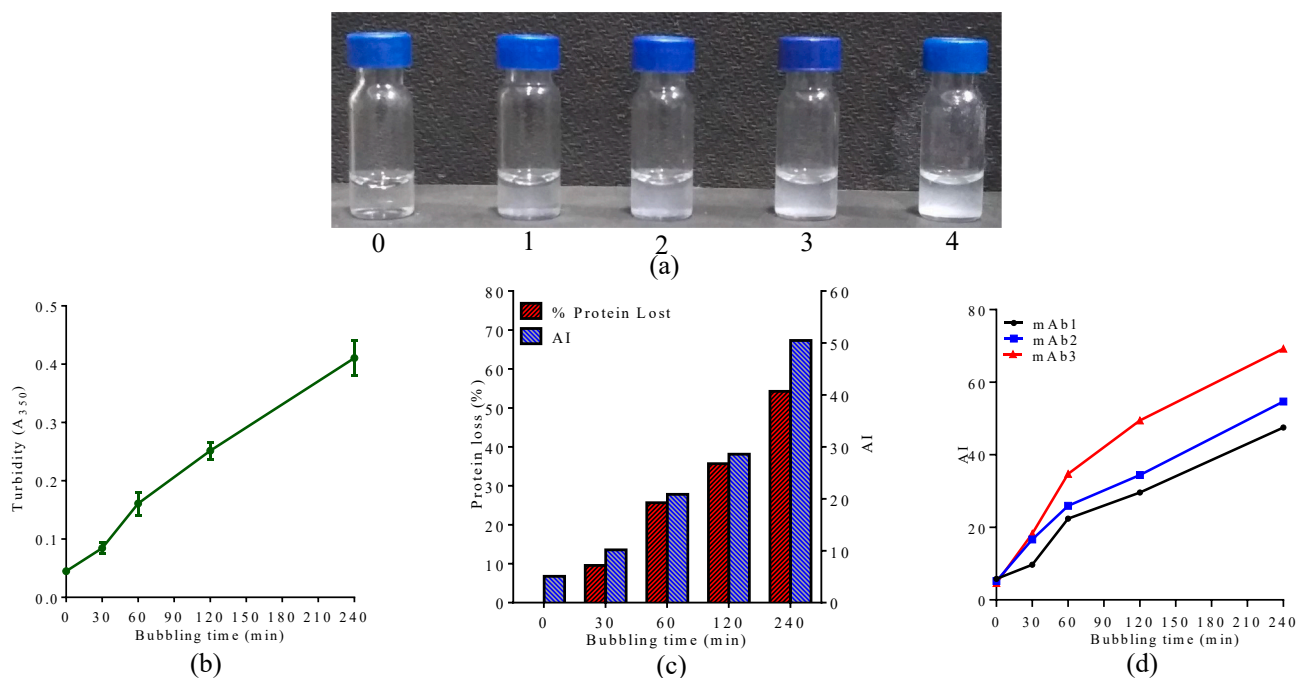


**Fig. 2.** Samples exposed to interfacial agitation through bubbling for up to 240 min with a sample volume of 500  $\mu$ L, mAb concentration of 1 mg/mL at 37  $^{\circ}$ C and an air flow rate of 11.5 mL/min, as detected for mAb1 by (a) visual observation, where 0 represents sample not subjected to any stress and 4 is the sample stressed for 240 min. The graph in (b) shows turbidity ( $A_{350}$ ) obtained at different time points and (c) shows aggregation index (AI, calculated from  $A_{350}$  and  $A_{280}$ ) and protein loss (%) (in the supernatant, cf. section 2.5), and (d) is the comparison of AI for mAb1, mAb2 and mAb3 samples.

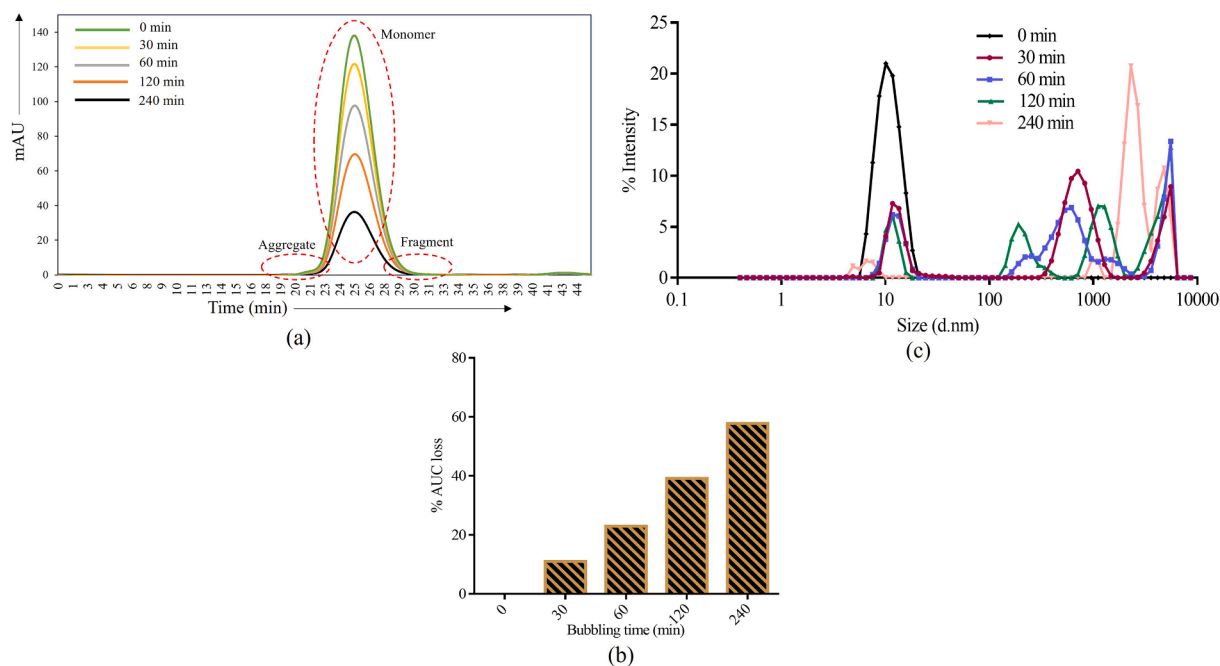


**Fig. 3.** (a) SEC chromatograms of supernatants of mAb1 sample obtained using Superdex 200 column. (b) The % loss of AUC in SEC chromatogram for mAb1 as function of bubbling time. (c) DLS results of mAb1 samples subjected to bubbling. The data is shown for 500  $\mu$ L of sample containing 1 mg/mL mAb stressed at 37  $^{\circ}$ C and 11.5 mL/min air flow rate for different time up to 240 min.

whereas in case of Superdex 75 column, the elution profile for monomer was obtained at 16.82 min. In Superdex 200 column, the area under elution profile integrated up to 22 min represented aggregate fraction, the area under the profile from 22 to 31 min represented monomer and the area under the profile obtained after 31 min represented fragments. Superdex 200 has an optimal separation range from 10 kDa to 600 kDa. In case of Superdex 75 column, the area under elution profile up to 16

min represented aggregates, area under the peak from 16 to 19 min represented monomer and the area under the profile beyond 19 min showed the presence of fragments. Superdex 75 shows an optimal separation range from 3 kDa to 70 kDa [19–21]. The AUC corresponding to aggregates and fragments were integrated to obtain the percentage of aggregates and fragments in the supernatant fraction of the sample (SI Fig. 3a). The initial mAb1 samples had relative monomer and aggregate

contents of 98.96% and 1.04%, respectively, when analyzed by Superdex 200 column. The same sample when analyzed by Superdex 75 column showed a fragment content of 1.19%. The SEC profiles of the supernatants of the stressed samples analyzed by Superdex 200 column is shown in Fig. 3a. It can be observed that the AUC got reduced with bubbling time. The percentage decrease in AUC is shown in Fig. 3b. A similar trend in the reduction in AUC was observed with Superdex 75 column (SI Fig. 3b). The relative percentages of aggregates, monomers and fragments remained almost constant throughout the bubbling time (240 min), see Table 1a & 1b. In contrast, the control samples did not show any changes in aggregation profile and protein recovery (SI Fig. 3c & 3d), indicating that incubating the mAb samples at 37 °C alone did not result in aggregation.

DLS can estimate the size of aggregates up to about 5 µm [20]. The plot of intensity against size shows that the size distribution of aggregates ranged towards the upper limit of the instrument and the Z-average diameter was > 10 µm for all the samples stressed from 30 min to 240 min (Fig. 3c). The presence of particulate aggregates >10 µm and the high polydispersity made DLS incapable of accurately determining the aggregate size distribution of the stressed samples. In case of control samples, DLS did not detect any changes in the particle size distribution, indicating that the samples were stable (SI Fig. 3d). The supernatants of the stressed samples were also analyzed by DLS. The data show that the mean size of proteins in the supernatant sample did not change significantly, as the Z-average ranged between 10.8 and 11.6 nm and the size distribution graph showed only one peak at about 10–11 nm, which is consistent with the SEC data.

The aggregate size in the sub-visible and visible range was analyzed by digital optical microscopy at 4x magnification. A representative image of a sample stressed for 120 min is shown in Fig. 4a, where the aggregates can be observed as dark spots against a bright background. A sample image for each time point is shown in Fig. 4b–4e, which shows the presence of dark coloured aggregates. It can be observed that the number of visible aggregates per image increased with time, indicating progressive formation of particles. The sample not subjected to any stress and the samples incubated at 37 °C without bubbling did not show any particulate aggregates.

The images of samples subjected to stress were subjected to an image processing algorithm (see SI Fig. 3e for a representative pixel distribution plot). The output binary images obtained after processing the raw images (shown in Fig. 4b–4e) are shown in Fig. 4f–4i, in which the aggregates can be seen as white particles against a black background. The x and y axis in the binary image correspond to the number of pixels along its length and height. Likewise, the output images for all the images obtained at all the time points were obtained and the size distribution of aggregates was obtained from the white particles. Aggregates having average diameters of 2.75 µm onwards were detected using our

**Table 1**

Percentage of aggregates and monomers in supernatant containing mAb1 obtained by SEC using Superdex 200 column is shown in (a). The amount of fragments was determined by Superdex 75 column and is shown in (b).

(a)		
Bubbling time	% Aggregates	% Monomer
0	1.04	98.96
30	1.20	98.80
60	2.01	97.99
120	0.80	99.20
240	0.85	99.15
(b)		
Bubbling time	% Fragments	
0	1.19	
30	1.37	
60	1.50	
120	1.24	
240	1.32	

algorithm. Aggregate size distributions of unstressed samples, control samples and empty slide (C-chip) were not obtained. The aggregate size distribution showed diameters ranging from 2.75 µm to 40 µm for samples up to 60 min and up to 100 µm for further time points, confirming the presence of sub-visible and visible aggregates (Fig. 4j–4m). The average diameter of aggregates obtained by our algorithm ranged from 5 to 9 µm. Hence, it can be concluded that the samples contained aggregates beyond the analysable range of SEC and DLS. From the size distribution and visual analysis, it can be concluded that a temperature of 37 °C, air flow rate of 11.5 mL/min, PBS and a sample volume of 500 µL resulted in rapid aggregation of the three different mAbs.

### 3.4. Structural characterization

Subjection of mAb samples to interfacial agitation resulted in the formation of sub-visible and visible aggregates. The aggregates and remaining monomers in samples subjected to stress might have altered secondary and tertiary structures. Hence, samples were analyzed via various spectroscopic tools, including (intrinsic and extrinsic) fluorescence spectroscopy, (near and far-UV) CD spectroscopy and ATR-FTIR. The stressed samples, supernatants, pellets and control samples were analyzed.

The samples were analyzed by intrinsic fluorescence spectroscopy for monitoring the changes in tertiary structure. The emission spectra for controls, samples subjected to stress and their supernatants were obtained and were subjected to smoothing. The sample not subjected to any stress had a maximum emission intensity wavelength ( $\lambda_{max}$ ) of 332 nm. In case of samples incubated for 240 min at 37 °C without subjecting to air/liquid bubbling interfacial stress, the  $\lambda_{max}$  and the fluorescence intensity remained constant, indicating a lack of conformational changes (SI Fig. 4a). A similar trend was seen for the supernatant samples, indicating that the soluble IgG fraction did not undergo conformational changes either (SI Fig. 4b). However, a red-shift up to 4 nm was observed for stressed samples, indicating enhanced exposure of tryptophan residues to the solvent (Fig. 5a). The red-shift did not consistently increase in time, which might be due to opposing effects during incubation or experimental error. Furthermore, for the supernatants of the samples subjected to stress, the fluorescence intensity decreased with bubbling time, which could be attributed to the decrease in soluble protein concentration (Fig. 5a).

The exposure of hydrophobic patches during aggregation was analyzed by extrinsic fluorescence spectroscopy [2,3,8]. The fluorescence emission spectra of ANS added to samples stressed between 0 and 240 min, its supernatants and control samples was analyzed. The control and unstressed samples showed emission spectra of minimum intensity for all the samples as compared to the stressed ones. In case of samples subjected to interfacial agitation, the fluorescence intensity and blue shift increased with time, with sample stressed for 240 min showing the highest intensity and blue shift (Fig. 5b). The plot of emission intensity at 505 nm against time for stressed and control samples are shown in SI Fig. 4c, where the intensity increased with time for samples stressed by air bubbling, with sample stressed at 240 min showing maximum intensity, thereby indicating exposure of hydrophobic patches with time. A similar trend of extrinsic emission spectra was obtained for mAb2 and mAb3 subjected to interfacial agitation through bubbling stress. Similar findings for increased intensity of ANS emission spectra are shown in other studies [2,3,8,13,26].

The secondary structure of the residual protein in the supernatants was monitored by using far-UV CD spectroscopy. The spectrum of unstressed mAb1 sample showed a negative maximum at 218 nm, passed through zero at 210 nm and had a positive maximum at 202 nm. The spectrum is characteristic of a high  $\beta$ -sheet content, as expected for a native mAb. The spectra corresponding to supernatants of samples subjected to bubbling are shown in Fig. 6a. All the spectra showed a similar intensity of positive maxima and negative minima, and passed through zero at 210 nm. The spectra of supernatant obtained at 240 min

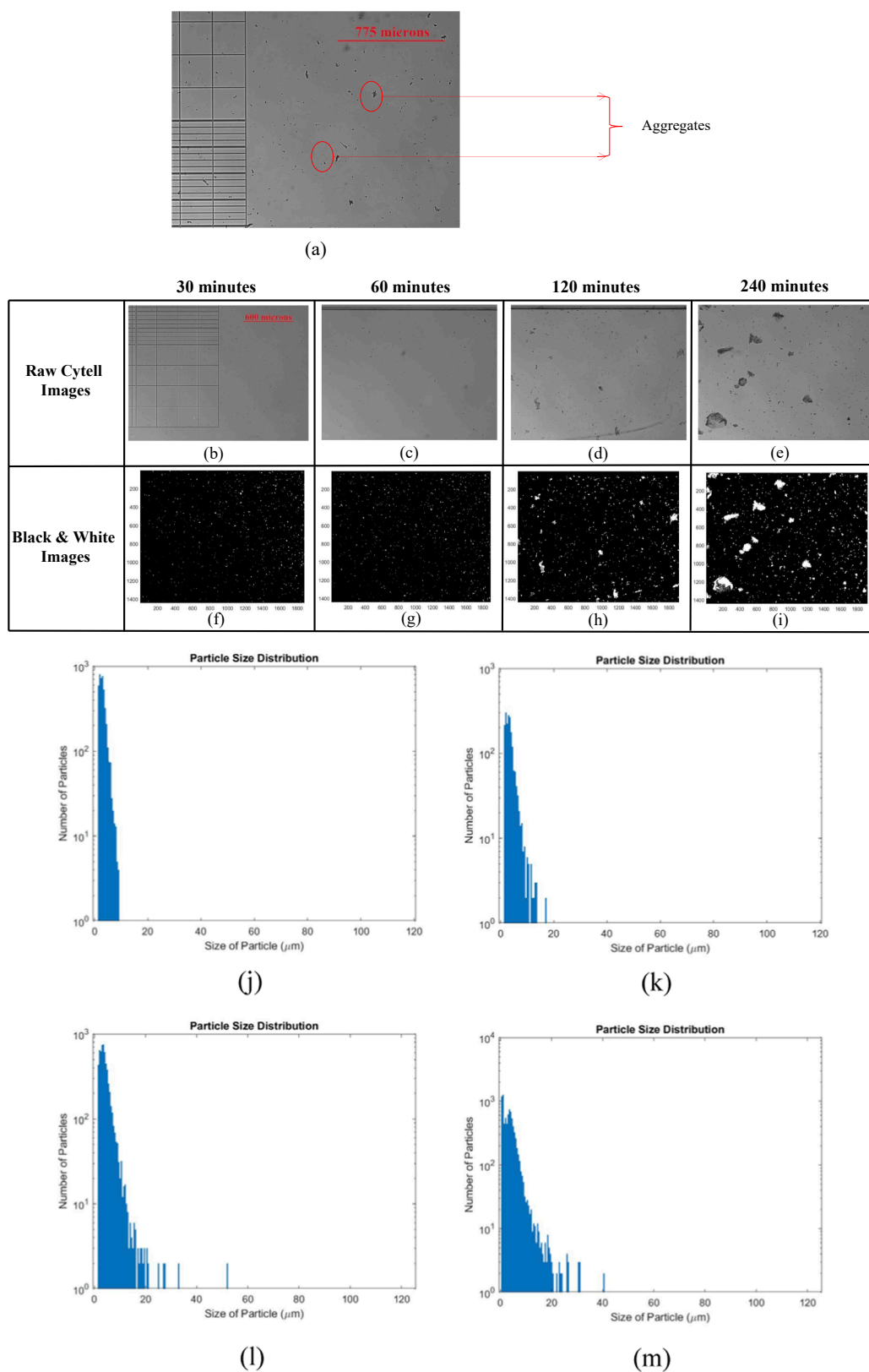


**Fig. 4.** Digital microscopy images for mAb1 samples subjected to interfacial agitation stress: (a) A representative image showing aggregates and background of sample containing mAb (500  $\mu\text{L}$  of 1 mg/mL mAb in PBS stressed for 120 min at 37 °C and 11.5 mL/min air flow rate). Images of samples subjected to bubbling (500  $\mu\text{L}$  of 1 mg/mL mAb in PBS at 37 °C and 11.5 mL/min air flow rate) for (b) 30 min, (c) 60 min, (d) 120 min and (e) 240 min. The binary image obtained after the processing the images for 30 min is shown in (f), 60 min in (g), 120 min in (h) and 240 min in (i). The size distribution of aggregates in the set of acquired images for the samples subjected to stress for 30 min is shown in (j), 60 min in (k), 120 min (l) and 240 min (m).

showed no major spectral changes, but a slightly more positive maximum at 210 nm and negative maximum at 218 nm. Furthermore, the far-UV CD spectra of control samples showed similar spectra (SI Fig. 5a). Overall, the far-UV CD spectra indicate that the secondary structure of the mAb in the supernatant was retained after the samples

were subjected to bubbling stress.

The tertiary structure of mAb in the supernatant sample was monitored by using near-UV CD spectroscopy (260–320 nm). The region of 260–320 nm depicts the side chain of aromatic residues. The spectrum of sample not subjected to any stress had a positive peak at 295 nm



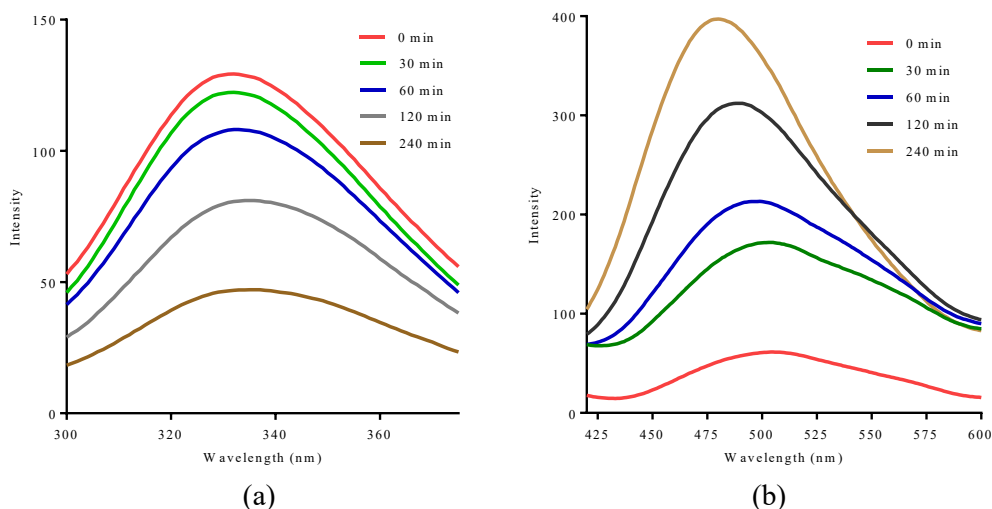


**Fig. 5.** Intrinsic fluorescence emission spectra of mAb1 samples exposed to bubbling for up to 240 min at 37 °C is shown in (a). Extrinsic fluorescence emission spectra of mAb1 samples exposed to bubbling for up to 240 min at 37 °C obtained with 10 μM is shown in (b).

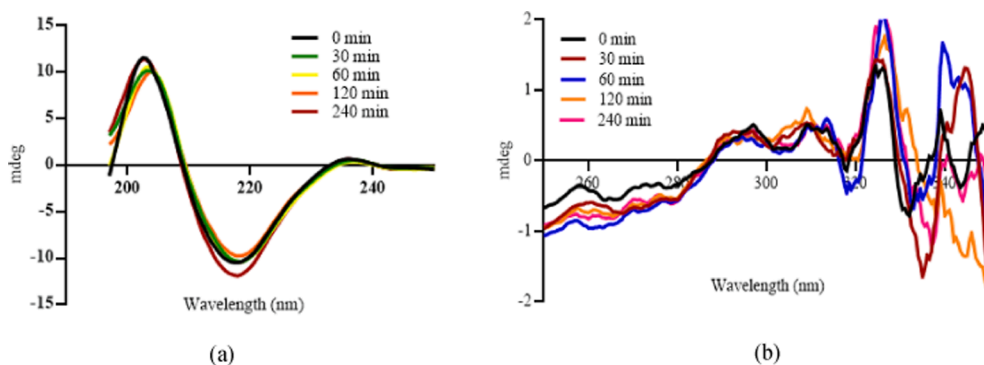


**Fig. 6.** (a) Far-UV CD spectra and (b) near-UV CD spectra of supernatants of mAb1 samples exposed to bubbling for up to 240 min at 37 °C.

(tryptophan) and a negative band in the range of 250–290 nm (tryptophan and tyrosine). The near-UV CD spectra of supernatants of samples subjected to stress are shown in Fig. 6b. Apart from some minor differences beyond 320 nm, all the spectra showed a similar profile. The near-UV CD spectra of control samples showed similar spectra, which indicates unaltered tertiary structure (SI Fig. 5b). In conclusion, significant structural changes were not detected by far-UV CD and near-UV CD spectrum for the supernatants of the samples stressed by interfacial agitation through bubbling.

The secondary structure of aggregates was analyzed by using FTIR spectroscopy. Samples containing 4 mg/mL (instead of 1 mg/mL) of IgG were stressed by bubbling to generate enough aggregates to be analyzed by FTIR. The stressed sample was then centrifuged, and the pellets were collected in sufficient quantity subjected to air-drying. Further, the supernatant of the samples was collected and concentrated. The pellet, unstressed and stressed sample, and the supernatant were subjected to ATR-FTIR spectroscopy. The spectra between 1600 and 1700  $\text{cm}^{-1}$  were obtained after normalization, blank subtraction, second derivative and smoothing (SI Fig. 6) and showed that the spectra were similar in case of unstressed sample, supernatant, and stressed sample. The spectra of pellets were changed mildly, indicating possible changes in the secondary structure of aggregated IgG.

### 3.5. Cell-based activity

The stressed sample containing mAb2 underwent further analysis with ADCC and CDC assays. mAb2 is known to kill CD20 + B cells by

ADCC. In ADCC, the effector cells are activated through the binding of the cell receptors to the Fc domain of the mAb. The ADCC assay involves the binding of a fully functional Fab domain of the mAb to the target cell (Raji cell) and binding of the Fc domain to the effector cells, which triggers the release of lytic proteins triggering the death of the target cell. The relative potency (ADCC) of mAb2 samples containing aggregates and controls in comparison to the unstressed sample obtained is shown in Table 2. In case of samples containing aggregates, the potency steadily dropped with increasing bubbling time to 0.61 at 240 min. In case of control samples, the potency ranged from 0.9 to 1 for all the samples (Table 2), indicating an unchanged biological activity. In case of CDC, the complement cascade triggers the formation of membrane attack complex which triggers causes the death of target cells. A trend similar to ADCC was observed for the CDC assay for the aggregated and control samples (SI Table 1). In case of supernatants of samples subjected to stress, the relative potency decreased with time, which can be

**Table 2**  
ADCC of stressed samples with aggregates and control samples containing mAb2.

Sample at 37 °C Time (min)	ADCC of Aggregates		ADCC of Controls	
	IU/mL	Std. Dev.	IU/mL	Std. Dev.
0	1.00		1	
30	0.91	0.025	0.95	0.04
60	0.83	0.04	0.96	0.03
120	0.72	0.015	0.95	0.02
240	0.61	0.03	0.93	0.04

attributed to increasing protein loss and formation of aggregates. Finally, it can be concluded that the potency decreased on increasing the duration of bubbling stress.

### 3.6. Impact of various parameters on aggregation

The protein concentration, excipients, temperature, volume, and headspace may influence the extent of aggregation upon interfacial stress [3,6,8,13]. Further, the intensity of interfacial agitation through bubbling might vary. Hence, the impact of air/liquid interfacial bubbling stress was investigated at varying protein concentration, sample volume, temperature, air flow rate and in the presence of various additives. After applying bubbling stress, samples were observed visually following the experimental determination of protein loss in the supernatant and turbidity. The turbidity was determined using  $A_{350}$ . The amount of protein in the supernatant was analyzed as protein loss (%), which was calculated using equation (2). 500  $\mu$ L of sample in PBS was stressed for 240 min at 37 °C, unless mentioned otherwise. In this section too, the results for mAb1 are described. MAb2 and mAb3 showed a similar trend.

#### 3.6.1. Protein concentration

The samples containing mAb1 were subjected to stress at a protein concentration of 1, 2, 4 and 8 mg/mL for different time points up to 240 min. The change in the turbidity and the amount of protein lost were inversely related to protein concentration, as shown in Fig. 7a-7b. It was found that the turbidity was the highest for the sample having the lowest mAb concentration: the stressed sample having 1 mg/mL of mAb was more turbid than sample containing 2 mg/mL of mAb, which was more turbid than stressed samples having 4 mg/mL and 8 mg/mL of mAb. The protein loss in the supernatant showed a similar trend as turbidity, as samples with the highest mAb concentration of mAb showed the least relative loss of soluble proteins at all time points. At the end of 240 min, samples with 1 mg/mL of mAb had lost the highest (56.75%) percentage of proteins, whereas samples with 2, 4 and 8 mg/mL of mAb had lost only 17.18, 12.4 and 5.25% of proteins. Hence, it was concluded that during interfacial agitation through bubbling at 37 °C, the rate of protein degradation is inversely proportional to the mAb concentration.

#### 3.6.2. Sample volume

Samples containing 1 mg/mL of mAb1 with a sample volume of 0.125, 0.25, 0.5, 1 and 2 mL were subjected to bubbling for 240 min at an air flow rate of 11.5 mL/min. The turbidity and the percentage of protein loss decreased on increasing the sample volume from 0.125 mL

to 2 mL (Fig. 8a). This result was expected, as at constant bubbling rate the interfacial area to bulk sample volume ratio becomes larger with decreasing sample volume, which was shown before to increase the aggregation rate [22]. Moreover, samples with a lower volume showed an increased tendency for whirling and splashing and hence the interaction of IgG with the air/liquid interface increased [12]. In conclusion, the sample volume had a significant impact on the conversion of soluble IgG into particulate aggregates.

#### 3.6.3. Temperature

The influence of temperature ranging from 4 to 75 °C was examined on the interfacial stability. To that end, samples containing 1 mg/mL of mAb1 at a sample volume of 500  $\mu$ L were exposed to bubbling stress at 4, 25, 37, 50 and 75 °C for 240 min, resulting in a higher turbidity and protein loss with increasing temperature (Fig. 8b). When the temperature was beyond 50 °C, the samples became highly turbid and lost > 85% of protein. But at 4 °C, the sample was barely turbid and had lost only 13.75% of protein after 240 min.

#### 3.6.4. Additives

The impact of the presence of silicone oil (1.5% v/v), PS80 (0.001% v/v) and PS20 (0.001% v/v) was investigated for interfacial agitation for 240 min at 11.5 mL/min (or pump speed of 5 rpm) and 37 °C. The turbidity and protein loss were calculated for all the samples and was compared to the sample subjected to stress without the presence of any additives (Fig. 8c). In the figure, sample marked as none indicates the one subjected to interfacial bubbling without the presence of any surfactants or silicone oil, and the one marked as control indicates sample incubated at 37 °C for 240 min without any interfacial agitation through bubbling. It was found that in the presence of silicone oil, the turbidity and protein loss increased. In contrast, in the presence of PS80 and PS20, the turbidity and protein loss were reduced.

#### 3.6.5. Bubbling rate

The turbidity and the percentage of lost proteins were monitored for samples containing 1 mg/mL of mAb1 subjected to interfacial agitation at different air flow rates up to 17.25 mL/min or the pump rpm of 7.5 for 240 min at 37 °C. Increase in the air flow rate resulted in a greater number of air bubbles, increasing the of air/liquid interfacial agitation per unit of time; along with increased agitation this likely led to accelerated the interaction of proteins in the bulk to interfaces and vice versa. Hence, as expected, there was an increase in protein loss in the supernatant and turbidity on increasing the air flow rate (Fig. 8d). Hence, suitable designing of equipment and controlled flow patterns are

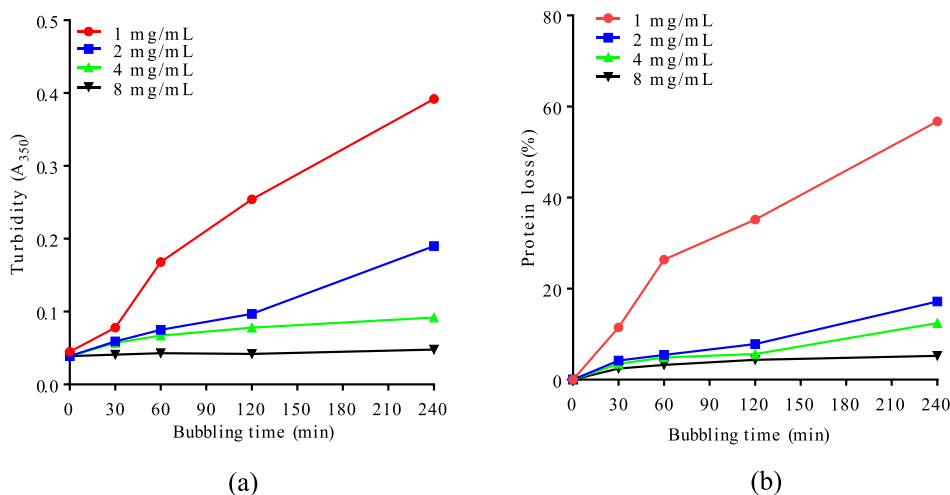
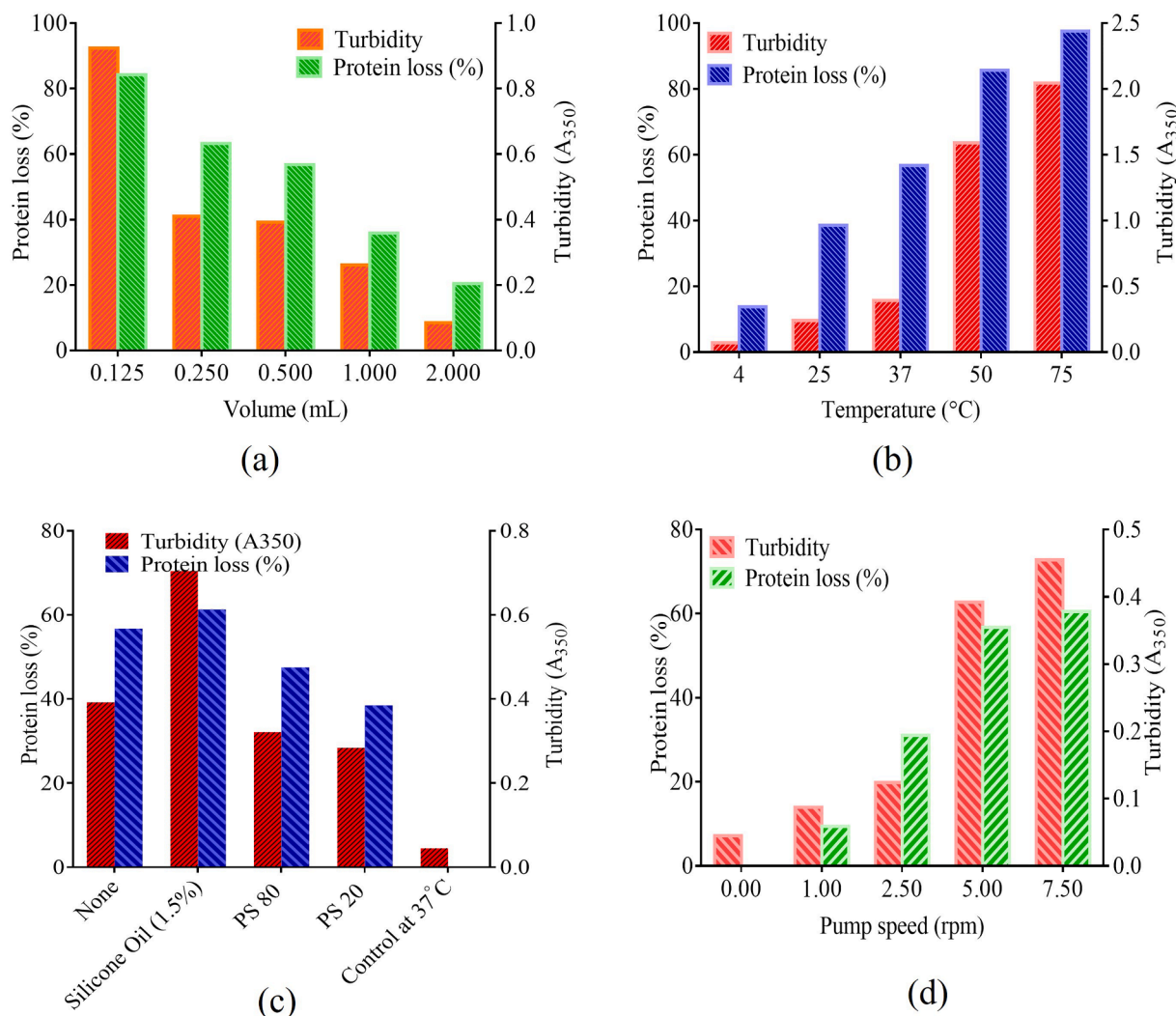


Fig. 7. Effect of mAb1 concentration on (a) turbidity and (b) protein loss (%) during air/liquid interfacial agitation through bubbling. 500  $\mu$ L of sample containing mAb of concentration ranging from 1 to 4 mg/mL in PBS was stressed for 240 min at 37 °C and air flow rate of 11.5 mL/min.



**Fig. 8.** Effect of (a) sample volume, (b) temperature, (c) presence of silicone oil or polysorbate and (d) bubbling rate on the stability of 1 mg/mL mAb1 in PBS exposed to bubbling for up to 240 min, as measured by turbidity ( $A_{350}$ ) and protein loss (%).

followed in the industries to reduce the impact of such kind of stresses.

#### 4. Discussion

Exposure of mAb therapeutics to interfacial surfaces is known to affect the critical quality attributes of the product [8]. Various reports have shown that the exposure of air/liquid interfacial surfaces along with mechanical stress such as shaking, stirring, and agitation on samples containing mAb has been detrimental to its stability [3,12–14]. Air/liquid interfacial stress in the form of bubbling occurs at multiple occasions, from cell culture to handling and administration of the drug product [4,7,8,11,13]. The conditions responsible for air/liquid interfacial stress might be different during various stages. For example, in case of cell culture, aeration in the form of air bubbles occurs from the sparger [23]. In downstream processing, the process of ultrafiltration/diafiltration could expose the proteins to multiple pump passes, recirculation, and mixing, thereby protein molecules undergoing interfacial stress. Further, sudden shaking and jerking of the products during storage, handling and administration can lead to air/liquid interfacial and agitation stress due to bubbling [8]. Air/liquid interfaces in the form of headspace are found during cell culture, purification, and storage in vials, syringes, stainless steel containers and plastic bags [8,12,15]. In the present study, forced degradation studies were carried out to investigate the aggregation behaviour of three mAbs in the presence of

air/liquid interfacial agitation in the form of bubbling. The conditions were chosen such that the mAb could rapidly degrade as compared to the degradation due to stirring, shaking, pumping and vortexing studies mentioned in the literature [2–4,8,13–17]. Further, the temperature of 37  $^{\circ}C$  represented a possible increased temperature which the sample containing mAb might be exposed to if taken away from its storage conditions in many of the geographical areas across the world. 37  $^{\circ}C$  the temperature during cell culture and it also represents the body temperature which the mAb faces after it is administered to the patient [5,7,8,23]. There are various approaches by using specialized equipments such as jacketed miniature reactor, Langmuir trough, micro tensiometer, friability testing apparatus, concentric-cylinder shear devices and rotating-disk reactors, other types of pumps such as piston and diaphragm pump are mentioned by different researchers [9,12–14,16,22,24,25,30–32]. Our strategy of generation of aggregates was effective, simple and reproducible. The current study could serve as an effective means to screen novel excipients, molecule screening, setting-shelf life and formulation development. The mAb samples subjected to interfacial agitation through bubbling were characterized by visual, sized-based, structural and functional analysis. The impact of protein concentration, sample volume, bubbling intensity, temperature, silicone oil, PS80 and PS20 were further investigated.

The samples subjected to stress became increasingly turbid with time, along with increases in AI and protein loss in the supernatant as

has also been reported by other researchers [2,3,8,12,13]. The conversion of IgG monomers into sub-visible and particulate aggregates on application of stress was the main reason. Findings similar to the current study have been reported by researchers who have subjected protein samples to air/liquid interfacial and shear related stresses, such as stirring, cavitation, shaking, filling, and recirculation [3,9,12–14]. Size analysis by SEC did not reveal the presence of any oligomers and fragments, and this might be due to the rapid conversion of monomers in the sample to aggregates that were beyond the analysis range of SEC such as sub-visible and visible aggregates. Researchers have demonstrated both the presence as well as absence of oligomers on application of similar stress. For example, Kiese et. al. 2007 have reported the presence of oligomers after applying shaking stress on 10 mg/mL of antibody of 5.3 mL sample volume. In the same study by Kiese et. al. 2007, application of stirring stress under identical conditions did not result in the formation of oligomers. However, the sample did turn turbid and exhibited presence of sub-visible and visible aggregates on applying both the stresses. In another study, Treuheit et al., 2002 reported presence of oligomers when the proteins were subjected to shipping related agitation stress. The type, extent of aggregation and the nature of aggregates are known to depend on the type of protein, its primary and higher order structure, formulation, intensity, and type of stress [7,11–13,22]. In our investigation, DLS and image processing were performed to confirm the presence of aggregates in the sub-visible and visible range and there are various literatures which showed that the sub-visible aggregates are highly immunogenic [5]. The processing of brightfield images was done by using a novel image processing algorithm. The difference in contrast between aggregate and background was utilised to analyze the images of brightfield microscopy. MAb2 and mAb3 subjected air/liquid interfacial agitation through bubbling showed images and size distribution trend similar to that of mAb1. Samples not subjected to any stress and the samples incubated at 37 °C without air/liquid interfacial agitation through bubbling did not show any particulate aggregates and hence their images were not analyzed (see SI Fig. 3f, an image of control sample obtained a higher magnification). The images of blank buffer (PBS) and empty slides were also acquired and showed the absence of any particulate aggregates similar to SI Fig. 3g. Further, some of the images being processed had air bubbles, which were removed accordingly during analysis. Among the processed images, the presented output was limited to the acquired images and hence the results might not be the exact quantitative representation of the entire sample. Further, the aggregates, and non-protein particles (in any, that would have crept in was not analyzed using the algorithm. A more accurate quantitative determination of size and particle number can be done by using techniques such as light obscuration, flow-based imaging, resonant mass measurement, and nanoparticle tracking analysis. Apart from our findings, several researchers have reported the presence of nano- and micron-sized particles due to shredding of sample containers and tubing upon subjecting the samples to similar stress [24,25]. However, the presence of non-protein particles was not considered in our study and further in-depth characterisation is required to analyze the same.

Stressing the samples by interfacial agitation through bubbling resulted in aggregates with altered higher order structure, as was evident from spectroscopic analysis. The results indicated the exposure of hydrophobic patches in the aggregates, changes in the environment around aromatic amino acids and altered secondary structure. Similar structural changes on stressing the samples by interfacial stresses such as stirring, and shaking have been reported in the literature [3,9,12–14,16]. An in-depth evaluation of structural changes was not carried out in this study. Interestingly, near-UV and far-UV CD spectroscopy of supernatants showed that the structure of proteins in the supernatants was not perturbed. This indicates that partially unfolded intermediates, if formed, might be so unstable that they were rapidly converted into sub-visible and visible aggregates.

The protein concentration is an important variable affecting aggregation [2,3,7]. The concentrations of IgG vary during the various

production stages, from upstream processing until formulation [4,7,23]. In this study, the relative amount of protein loss became lower upon increasing the concentration. Similar findings have been reported by other researchers. For example, the protein under consideration was stressed at 24000 rpm in presence of air/liquid interface at different concentrations of 0.5, 2 and 5 mg/mL. At 20 min, it was found that the sample with 0.5 mg/mL of protein had most maximum amount of monomers [17]. In another study, the aggregation tendency of protein got reduced when the concentration was increased to 8 and 25 mg/mL [9]. The possible reason has been stated that even when protein concentration was increased, the interfacial area remained constant, and it could degrade more percentage of proteins in the bulk when the concentration was lower [9]. Yet another study has reported that when proteins at 1, 5 and 10 mg/mL were exposed to shaking, vortexing and shipping related agitation, the sample with least concentration underwent maximum aggregation [10]. The possible reason behind this trend was stated as the ratio of air/liquid interfacial stress to protein concentration, i.e, when the concentration was lower, the ratio was high and resulted in increased aggregation [10].

The volume of sample containing IgGs can range from hundreds of litres during cell culture to less than a mL in the final formulation. In our study, the protein loss and turbidity decreased with increasing sample volume, which is likely due to the concomitant change in the interfacial area/volume ratio. The volume of the eppendorf tube in which the aggregation was carried out was constant throughout. This is in line with studies on the impact of headspace on aggregation [8,12,13]. A lack of headspace results in a highly reduced degradation of proteins on exposure to mechanical stress.

From production up until administration, mAbs are exposed to various temperatures. For example, a temperature of 37 °C is typical during cell culture and a possibility during accidental exposure from its storage conditions, a drug substance may be stored frozen at –20 or –80 °C, whereas a drug product is typically stored at 2–8 °C before being warmed up to room temperature prior to administration [6,7,23,26]. In case of bubbling and other air/liquid interfacial stress, the IgGs are known to be adsorbed to hydrophobic interfaces. The possible temperature dependence of the adsorption of mAb to the air/liquid interface [8,12,13] as well as the higher degree of unfolding near the melting temperature [12,13] may together have been responsible for the increase in turbidity of the mAb samples observed in our study when interfacial stressing by bubbling was performed at 50 and 75 °C.

In prefilled syringes lubricated with silicone oil, proteins encounter liquid water/silicone oil interfaces. Proteins are known to get adsorbed to it and form a monolayer, which may lead to conformational perturbations resulting in aggregation [7,8,27]. In our experimental set-up, the presence of silicone oil indeed resulted in enhanced aggregation and turbidity. Agitation through bubbling most likely increased the interfacial area for the interaction of mAb to oil and could thereby accelerate degradation. Hence, use of silicone oil in primary packaging materials is a major challenge in the development, usage, commercialization, and long-term storage of proteins. Nowadays, silicone oil free syringes, or syringes with modified cross linked silicone oil and other coatings are being developed [8,27], which may help to mitigate the risk.

The degradation of IgG was reduced in terms of proteins loss and turbidity when the samples were subjected to bubbling in the presence of a surfactants, PS20 or PS80. These are non-ionic, amphipathic molecules and are known have protective action against bubbling and agitation [12–14]. These surfactants are known to have a higher surface activity than mAbs, which can result in competitive inhibition of mAb adsorption to the interface, thereby preventing aggregation [11–14]. Furthermore, the surfactants might interact with the exposed hydrophobic regions of the proteins to prevent aggregation [8,27].

There are various studies that show the formation of particulate aggregates using air/liquid interfacial stress [9,12–14,16,22,24,28–30], and in some of the studies, the influence of various factors affecting aggregation was different from the ones reported in the current study.



For example, in case of Weisbauer et al., 2021 and Bee et al., 2012, the concentration was either weakly dependent or not dependent on aggregation. In case of Wood et al., 2012, the particle formation was weakly dependent on temperature. This could be due to the underlying mechanism, protein concentration, intensity and nature of interfacial stress along with other additional stress related factors and nature of proteins. The possible cause of rapid degradation due to bubbling can be explained with various theories about the aggregation of proteins in the presence of air/liquid interfaces [8–10,12]. One of the most accepted explanations is depicted in Fig. 9. In the figure, a sample containing mAb subjected to air/liquid interfacial agitation is shown, whose enlarged view is shown using dotted arrows to show different stages involved in aggregation shown in Fig. 9a–9c. The transition from the stage shown in Fig. 9(a) to Fig. 9(c) is shown using straight line arrows.

Proteins are amphipathic molecules, and they are stable against local unfolding in the native state [31]. On subjecting the sample to air/liquid interfacial bubbling, the presence of air bubbles, headspace and monomers in the buffer is shown in Fig. 9a. The presence of air/liquid interfacial surface in a sample containing proteins results in their adsorption to the interfacial surface. As air is more hydrophobic than water, the interaction of proteins to the air/water interface can trigger the exposure of its hydrophobic patches. Such protein molecules in a partially unfolded state with the hydrophobic groups exposed to the exterior can form nuclei [8,12]. The exposed of hydrophobic patches and adsorption of partially unfolded mAb to air/liquid interface is shown in Fig. 9b. These can interact with other protein molecules and among themselves, resulting in attractive intermolecular interactions to form aggregates [13,25,32]. The aggregates formed are shown in Fig. 9c. Protein films formed at the interface can dislodge and break up due to various forces and the aggregates present in the bulk after dislodging of film can promote further aggregation [16]. Moreover, this interface-mediated aggregate formation can be further accelerated by movement of proteins at the interface through convective mass transfer through creation or destruction of the bubbles [22]. Hence, the combination of agitation and air/liquid interfacial surfaces enhances the formation of nuclei and accelerates rapid interaction of nuclei among themselves and between other protein molecules to form aggregates [8,13]. The intensity of agitation and the air/liquid interfacial area might vary depending on

various factors, resulting in different rates of aggregation. The rapid bubbling and agitation might also result in enhanced local heating and cavitation effects, i.e., the formation of tiny bubbles that collapse rapidly, creating shock waves along with extremely high temperatures, pressures, and turbulent conditions, leading to the IgG aggregation [13,14]. Further, there have been other proposed mechanism where the proteins at the interface forms compressible film, whose speed of compression affected the number of particulate aggregates. However, in this case, the proteins at the interface had native like confirmation [14]. Apart from air/liquid interfacial stress and agitation induced by bubbling, there might also be a possible impact of liquid/solid interface contributed by needle and Eppendorf tube wall during bubbling that could have contributed to rapid aggregation. In order to prevent the impact of such stresses and formation aggregates in mAb manufacturing, suitable process design and operation as well as formulation optimization is recommended [8,16].

## 5. Conclusions

The impact of rapid bubbling induced air/liquid interfacial surfaces and agitation was investigated at different conditions for the stability of samples containing therapeutic mAb. Rapid generation of aggregates in the sub-visible and visible range was observed. The stressed samples showed the absence of soluble oligomers. The aggregate-containing samples exhibited altered hydrophobicity and secondary structure. The structure of proteins in the supernatant was retained. Furthermore, the rate of aggregation strongly depended on the experimental conditions. Our strategy of generation of aggregates was effective, simple, reproducible, and cheap, and hence it could be an efficient way to generate aggregates for purposes such as mechanistic studies of protein aggregation, screening of novel excipients and protein formulation development. Moreover, the lack of any standard conditions for forced degradation studies in general enables any company or laboratory to develop similar set-ups for stress testing and degradation studies for mAbs and other biopharmaceuticals. As demonstrated in this study, the presented bubbling set-up allows a facile screening of the influence of several factors, such as temperature, protein concentration, sample volume, intensity of agitation and presence of silicone oil as well as

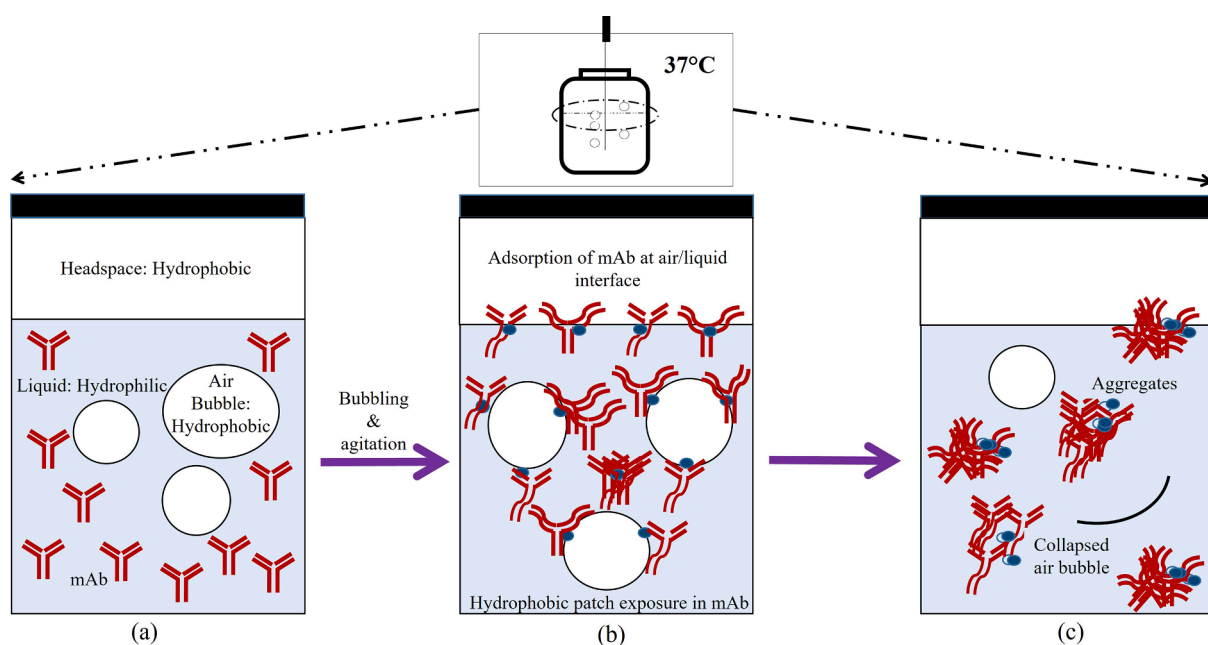


**Fig. 9.** Scheme of the putative mechanism involved in the aggregation of mAb in the presence of air/liquid interfacial agitation through bubbling. The presence of air bubbles, headspace and monomers in the buffer is shown in (a). Exposure of hydrophobic patches and adsorption of mAb to air/liquid interface is shown in (b). The aggregates formed are shown in (c).

formulation excipients and pH, on the sensitivity of proteins to air/liquid interfacial agitation stress.

#### CRedit authorship contribution statement

**Shravan Sreenivasan:** Conceptualization, Investigation, Methodology, Writing – original draft. **Wim Jiskoot:** Methodology, Writing – review & editing. **Anurag S. Rathore:** Supervision, Funding acquisition, Writing – review & editing.

#### Declaration of Competing Interest

The authors declare that they have no known competing financial interests or personal relationships that could have appeared to influence the work reported in this paper.

#### Acknowledgements

This work was funded by the Centre of Excellence for Biopharmaceutical Technology grant from the Department of Biotechnology, Ministry of Science and Technology (number BT/COE/34/ SP15097/2015). SS acknowledges Council of Scientific and Industrial Research, New Delhi, for the award of SRF-fellowship (Award No. 09/086(1312)/2018-EMR-I). The authors acknowledge Dr. Rozaleen Dash, IIT Delhi, for her support with cell based assays and Deepak Sonawat, IIT Delhi, for image analysis.

#### Appendix A. Supplementary material

Supplementary data to this article can be found online at <https://doi.org/10.1016/j.ejpb.2021.08.010>.

#### References

- [1] A.S. Rosenberg, Z.E. Sauna, Immunogenicity assessment during the development of protein therapeutics, *J. Pharm. Pharmacol.* 70 (5) (2018) 584–594.
- [2] M.K. Joubert, Q. Luo, Y. Nashed-Samuel, J. Wypych, L.O. Narhi, Classification and characterization of therapeutic antibody aggregates, *J. Biol. Chem.* 286 (28) (2011) 25118–25133.
- [3] R. Bansal, R. Dash, A.S. Rathore, Impact of mAb Aggregation on Its Biological Activity: Rituximab as a Case Study, *J. Pharm. Sci.* 109 (9) (2020) 2684–2698.
- [4] J. den Engelsman, P. Garidel, R. Smulders, H. Koll, B. Smith, S. Bassarab, A. Seidl, O. Hainzl, W. Jiskoot, Strategies for the assessment of protein aggregates in pharmaceutical biotech product development, *Pharm. Res.* 28 (4) (2011) 920–933.
- [5] V. Filipe, W. Jiskoot, A.H. Basmeleh, A. Halim, H. Schellekens, V. Brinks, November. Immunogenicity of different stressed IgG monoclonal antibody formulations in immune tolerant transgenic mice, *MAbs* 4 (6) (2012) 740–752.
- [6] A. Singla, R. Bansal, V. Joshi, A.S. Rathore, Aggregation kinetics for IgG1-based monoclonal antibody therapeutics, *The AAPS Journal* 18 (3) (2016) 689–702.
- [7] T.K. Das, L.O. Narhi, A. Sreedhara, T. Menzen, C. Grapentin, D.K. Chou, V. Antochshuk, V. Filipe, Stress factors in mAb drug substance production processes: critical assessment of impact on product quality and control strategy, *J. Pharm. Sci.* 109 (1) (2020) 116–133.
- [8] J. Li, M.E. Krause, X. Chen, Y. Cheng, W. Dai, J.J. Hill, M. Huang, S. Jordan, D. LaCasse, L. Narhi, E. Shalav, I.C. Shieh, J.C. Thomas, R. Tu, S. Zheng, L. Zhu, Interfacial stress in the development of biologics: fundamental understanding, current practice, and future perspective, *The AAPS Journal* 21 (3) (2019), <https://doi.org/10.1208/s12248-019-0312-3>.
- [9] M. Duerkop, E. Berger, A. Dürauer, A. Jungbauer, Impact of cavitation, high shear stress and air/liquid interfaces on protein aggregation, *Biotechnol. J.* 13 (7) (2018) 1800062, <https://doi.org/10.1002/biot.v13.7.1002/1002/1002/1800062>.
- [10] M.J. Treuheit, A.A. Kosky, D.N. Brems, Inverse relationship of protein concentration and aggregation, *Pharm. Res.* 19 (4) (2002) 511–516.
- [11] M.R. Nejadnik, T.W. Randolph, D.B. Volkin, C. Schöneich, J.F. Carpenter, D.J. A. Crommelin, W. Jiskoot, Postproduction handling and administration of protein pharmaceuticals and potential instability issues, *J. Pharm. Sci.* 107 (8) (2018) 2013–2019.
- [12] S. Kiese, A. Pappengerger, W. Friess, H.-C. Mahler, Shaken, not stirred: mechanical stress testing of an IgG1 antibody, *J. Pharm. Sci.* 97 (10) (2008) 4347–4366.
- [13] T. Torisu, T. Maruno, Y. Hamaji, T. Ohkubo, S. Uchiyama, Synergistic effect of cavitation and agitation on protein aggregation, *J. Pharm. Sci.* 106 (2) (2017) 521–529.
- [14] E. Koepf, S. Eisele, R. Schroeder, G. Brezesinski, W. Friess, Notorious but not understood: how liquid-air interfacial stress triggers protein aggregation, *Int. J. Pharm.* 537 (1–2) (2018) 202–212.
- [15] A. Hawe, M. Wigggenhorn, M. van de Weert, J.H.O. Garbe, H.-C. Mahler, W. Jiskoot, Forced degradation of therapeutic proteins, *J. Pharm. Sci.* 101 (3) (2012) 895–913.
- [16] F. Grigolato, P. Arosio, Synergistic effects of flow and interfaces on antibody aggregation, *Biotechnol. Bioeng.* 117 (2) (2020) 417–428.
- [17] Y.-F. Maa, C.C. Hsu, Protein denaturation by combined effect of shear and air-liquid interface, *Biotechnol. Bioeng.* 54 (6) (1997) 503–512.
- [18] S.K. Panda, B. Ravindran, Isolation of human PBMCs, *Bio-protocol* 3 (3) (2013) 323.
- [19] L. Kågedal, B. Engström, H. Elégren, A.-K. Lieber, H. Lundström, A. Sköld, M. Schenning, Chemical, physical and chromatographic properties of Superdex 75 prep grade and Superdex 200 prep grade gel filtration media, *J. Chromatogr. A* 537 (1991) 17–32.
- [20] R. Bansal, S. Gupta, A.S. Rathore, Analytical platform for monitoring aggregation of monoclonal antibody therapeutics, *Pharm. Res.* 36 (11) (2019), <https://doi.org/10.1007/s11095-019-2690-8>.
- [21] S. Ravuluri, R. Bansal, N. Chhabra, A.S. Rathore, Kinetics and characterization of non-enzymatic fragmentation of monoclonal antibody therapeutics, *Pharm. Res.* 35 (7) (2018) 1–13.
- [22] S. Amin, G.V. Barnett, J.A. Pathak, C.J. Roberts, P.S. Sarangapani, Protein aggregation, particle formation, characterization & rheology, *Curr. Opin. Colloid Interface Sci.* 19 (5) (2014) 438–449.
- [23] Z. Xing, B.M. Kenty, Z.J. Li, S.S. Lee, Scale-up analysis for a CHO cell culture process in large-scale bioreactors, *Biotechnol. Bioeng.* 103 (4) (2009) 733–746.
- [24] C. Her, J.F. Carpenter, Effects of tubing type, formulation, and post pumping agitation on nanoparticle and microparticle formation in intravenous immunoglobulin solutions processed with a peristaltic filling pump, *J. Pharm. Sci.* 109 (1) (2020) 739–749.
- [25] A. Nayak, J. Colandene, V. Bradford, M. Perkins, Characterization of subvisible particle formation during the filling pump operation of a monoclonal antibody solution, *J. Pharm. Sci.* 100 (10) (2011) 4198–4204.
- [26] A. Hawe, J.C. Kasper, W. Friess, W. Jiskoot, Structural properties of monoclonal antibody aggregates induced by freeze–thawing and thermal stress, *Eur. J. Pharm. Sci.* 38 (2) (2009) 79–87.
- [27] R. Thirumangalathu, S. Krishnan, M.S. Ricci, D.N. Brems, T.W. Randolph, J. F. Carpenter, Silicone oil-and agitation-induced aggregation of a monoclonal antibody in aqueous solution, *J. Pharm. Sci.* 98 (9) (2009) 3167–3181.
- [28] J. Wiesbauer, R. Prassl, B. Nidetzky, Renewal of the air–water interface as a critical system parameter of protein stability: aggregation of the human growth hormone and its prevention by surface-active compounds, *Langmuir* 29 (49) (2013) 15240–15250.
- [29] C.V. Wood, V.I. Razinkov, W. Qi, E.M. Furst, C.J. Roberts, A Rapid, Small-Volume Approach to Evaluate Protein Aggregation at Air–Water Interfaces, *J. Pharm. Sci.* 110 (3) (2021) 1083–1092.
- [30] J.S. Bee, D.K. Schwartz, S. Trabelsi, E. Freund, J.L. Stevenson, J.F. Carpenter, T. W. Randolph, Production of particles of therapeutic proteins at the air–water interface during compression/dilation cycles, *Soft Matter* 8 (40) (2012) 10329–10335.
- [31] S.V. Thakkar, N. Sahni, S.B. Joshi, B.A. Kerwin, F. He, D.B. Volkin, C.R. Middaugh, Understanding the relevance of local conformational stability and dynamics to the aggregation propensity of an IgG1 and IgG2 monoclonal antibodies, *Protein Sci.* 22 (10) (2013) 1295–1305.
- [32] L.L. Sorret, M.A. DeWinter, D.K. Schwartz, T.W. Randolph, Protein–protein interactions controlling interfacial aggregation of rHL-1ra are not described by simple colloid models, *Protein Sci.* 27 (7) (2018) 1191–1204.